Whitmarsh, R.B., Sawyer, D.S., Klaus, A., and Masson, D.G. (Eds.), 1996
Proceedings of the Ocean Drilling Program, Scientific Results, Vol. 149

27. GEOCHEMISTRY OF METAMORPHOSED CUMULATE GABBROS FROM HOLE 900A, IBERIA ABYSSAL PLAIN[1]

Karl Seifert,[2] Ian Gibson,[3] Dominique Weis,[4] and Dale Brunotte[2]

ABSTRACT

Basement at ODP Hole 900A consists of metamorphosed cumulate gabbros with discontinuous foliation bands of recrystallized plagioclase and clinopyroxene containing a few large isolated porphyroclasts of strained plagioclase and clinopyroxene respectively. Locally the pyroxene has retrograded to fine-grained amphibole and other minerals and the retrograded cores are cut by multiple generations of veins. The alternating discontinuous felsic and mafic bands define a poorly developed foliation that is characteristic of high-grade metamorphism in ocean crust and quite distinct from high-grade continental metamorphism. The Hole 900A cumulate gabbros have very low concentrations of Zr (10-30 ppm) and other incompatible elements indicating little magma retention. Their geochemistry is similar to that of cumulate gabbros from the Mid-Atlantic and Southwest Indian Ridges. Rare earth element patterns are flat at 2X-4X chondrite with small positive europium anomalies. Spider diagrams reveal a secondary enrichment in the soluble large ion lithophile elements and U relative to less soluble incompatible elements. The association of K concentrations in alteration patches with amphibole indicates these elements were added by seawater during the hydrous retrograde metamorphism. Nd and Pb isotopic analyses indicate the gabbros were formed in an oceanic environment and the high positive initial ϵ_{Nd} values (>6 at 136.4 Ma) indicate a MORB origin. High Sr isotopic ratios and high U/Pb ratios reveal seawater alteration. Based on a rare earth element pattern using literature partition coefficients for plagioclase and clinopyroxene, the average parental magma for the Hole 900A cumulate gabbros resembles transitional MORB. These geochemical data provide evidence for the presence of an active mid-ocean ridge magma chamber in the Iberia Abyssal Plain region 136.4 Ma.

INTRODUCTION

Leg 149 of the Ocean Drilling Program (ODP) explored the ocean-continent transition (OCT) on the Iberia Abyssal Plain and its role in the opening of the Atlantic Ocean approximately 130 Ma ago. Leg 149 was the first of several legs in the Atlantic Ocean to study rifted-margin formation and evolution. Transects were chosen across both volcanic and nonvolcanic conjugate rifted margins with basement being the major drilling target to better define the nature of such margins and their role in the opening of the Atlantic Ocean. The Iberia Abyssal Plain was chosen as the best defined nonvolcanic rifted margin on the eastern edge of the Atlantic Ocean (Fig. 1), the geologically conjugate Newfoundland margin was to be drilled on a later leg. The Iberia continental margin consists of several topographically distinct regions. In the northern part of the margin continental crust extends seaward under shallow water as the 200 km by 150 km Galicia Bank. The Galicia Bank contains a series of isolated seamounts along its southern edge and is separated from Iberia by a broad submarine valley. The Iberia Abyssal Plain lies south of the Galicia Bank (Fig. 2). Here the continental margin has a straight narrow shelf and a steep continental slope. South of 40°N the slope is cut by numerous deep canyons and at 39°N the east-west Estremadura Spur separates the Iberia Abyssal Plain from the Tagus Abyssal Plain that forms the southern part of the Iberia continental margin. South of the Tagus Abyssal Plain the east-northeast Gorringe Bank marks the seismically active plate boundary between Eurasia and Africa.

Three main episodes of Mesozoic rifting marked the separation of the Iberia Margin from the Newfoundland Grand Banks. The first episode was a Triassic to Early Jurassic rifting phase that produced graben and half-graben structures in which evaporites were deposited (Wilson et al, 1989; Murillas et al., 1990). A second rifting event consisted of extension in Late Jurassic time. A third episode of Early Cretaceous extension marked the south-to-north breakup of Iberia from the Grand Banks (Boillot, Winterer, Meyer, et al, 1987; Whitmarsh et al., 1990; Pinheiro et al., 1992). These studies found that the OCT crust in this region is only about 4 km thick and is underlain everywhere by a continuous layer with a velocity near 7.6 km/s that is probably serpentinized mantle peridotite. Plate reconstructions of Iberia with Europe and North America are difficult because Iberia was alternately attached to Europe and Africa (Srivastava et al., 1990).

Leg 149 was designed, on the basis of geophysical data, to drill across the entire OCT from the oceanic to the continental edge of the Iberia rifted margin but instead found an ocean-continent gap at least 130 km wide. Geophysical studies by Whitmarsh et al. (1990), Beslier et al. (1993), and Whitmarsh et al. (1993) have defined the crustal characteristics used to target drill sites on the Iberia Abyssal Plain. The major drill targets on the Iberia Abyssal Plain were a series of basement highs (Fig. 3) beneath several hundred meters of sediment cover. At Hole 900A a series of fine-grained recrystallized and foliated metamorphic rocks of mafic composition were drilled. Primary textures were completely destroyed and the only chance to determine the genesis of these rocks rests in determining and interpreting their compositional characteristics. This study deciphers the primary igneous petrogenesis of the ODP Hole 900A metamorphosed mafic rocks rather than the nature of their subsequent metamorphism. Consequently, our samples were chosen from parts of the core with the cleanest recrystallized plagioclase and clinopyroxene assemblage, avoiding regions that were largely retrograded to amphibole and other hydrous minerals.

[1] Whitmarsh, R.B., Sawyer, D.S., Klaus, A., and Masson, D.G. (Eds.), 1996. *Proc. ODP, Sci. Results,* 149: College Station, TX (Ocean Drilling Program).
[2]Department of Geological & Atmospheric Sciences, Iowa State University, Ames, IA 50011, U.S.A. Seifert: kseifert@iastate.edu
[3]Department of Earth Sciences, University of Waterloo, Waterloo, Ontario N2L 3G1, Canada.
[4]Petrology-Chemical Geodynamics, Université Libre de Bruxelles, B-1050 Brussels, Belgium.

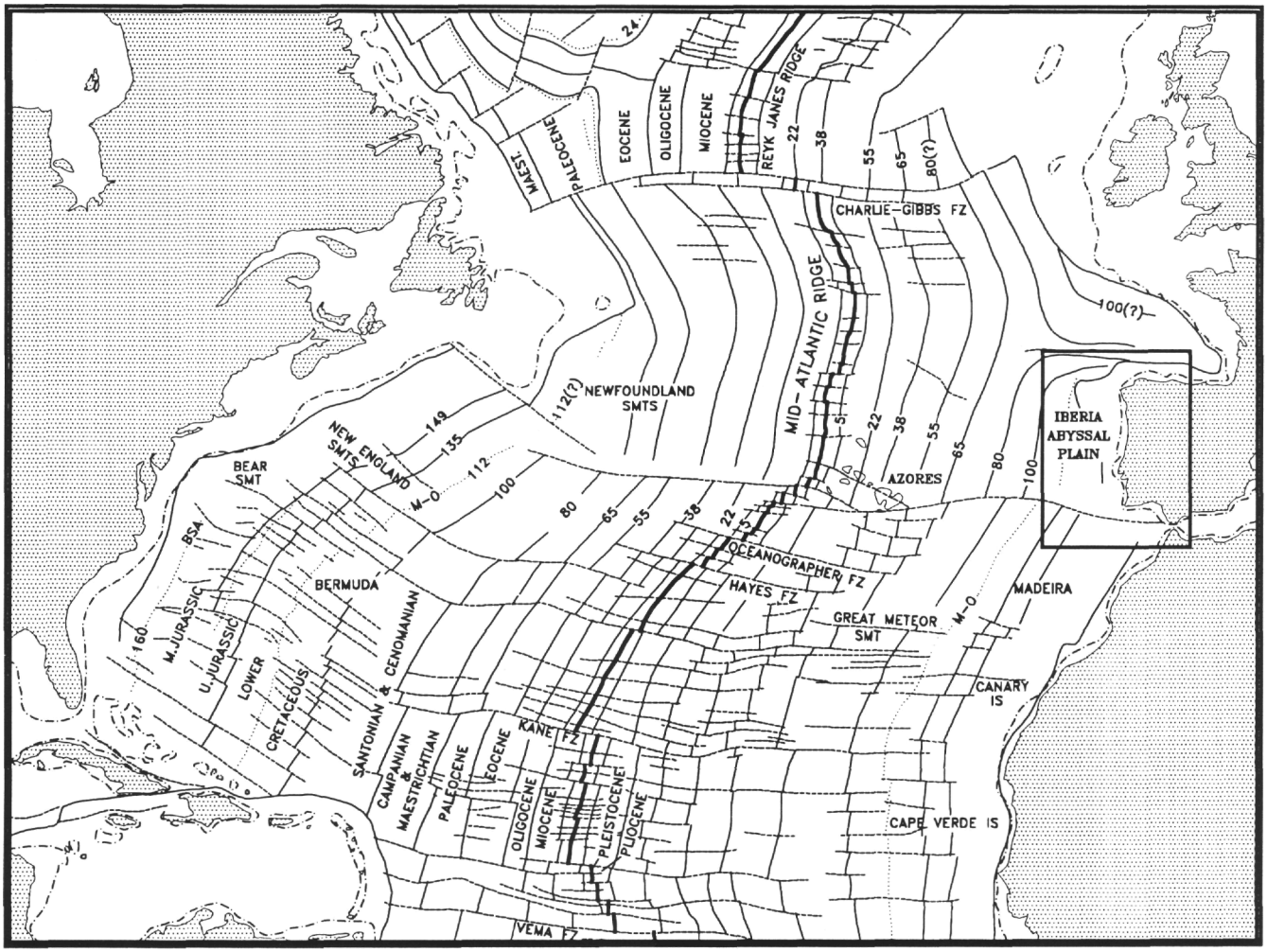

Figure 1. Map of the Atlantic Ocean showing the location of the Iberia Abyssal Plain (box) on the conjugate margin to Newfoundland and the Grand Banks. The map also shows isochrons (m.y.), fracture zones (dashed lines), and a few magnetic anomalies (dotted lines) in the reversal sequence. Modified from Vogt and Perry (1981).

ANALYTICAL TECHNIQUES

A variety of analytical techniques was used in order to obtain an accurate analysis of as many elements as possible. The major elements Si, Ti, Al, Fe, Mn, Mg, Ca, Na, K, and P were determined by inductively-coupled plasma (ICP) techniques, the oxidation state of Fe required a separate titration, and H_2O^+, H_2O^-, and CO_2 have been combined into loss on ignition (LOI). The LOI were not corrected for the O gain caused by oxidation of ferrous to ferric iron. Trace elements Ba, V, Cr, Ni, Zn, Cu, Pb, and Sr were also determined by ICP analysis. Fourteen rare earth elements (REEs), Sr, Ba, Th, Rb, Nb, Y, Hf, Ta, U, Pb, and Cs were determined by inductively-coupled plasma mass spectrometry (ICP/MS). All of the analyses were contracted to commercial laboratories, except for the ferrous iron titrations, which were done at Iowa State University. ICP analyses were obtained from commercial laboratories (Chemex and Acme) and ICP/MS and $^{18}O/^{16}O$ analyses were obtained from the GeoAnalytical Laboratory at Washington State University, Charles Knaack was the ICP/MS analyst. Accuracy of the ICP analyses was checked by including USGS standards BCR-1, BHVO-1 and NBS flyash 1633a as unknowns among the samples and repeated runs of the commercial laboratory in-house standards. Accuracy of the ICP/MS analyses was checked by a well characterized BCR-1 clone from the same quarry (BCR-P) and other in-house standards used at the Washington State GeoAnalytical Laboratory. Precision of both the ICP and ICP/MS analyses was estimated at 5% to 10% from duplicate runs of standards and several unknowns, except near the detection limit, which was 0.1X to 0.5X chondrite for trace elements run by ICP/MS. Trace elements run by both ICP and ICP/MS appear to have been more accurately determined by ICP/MS analysis and the ICP/MS data are preferentially reported.

The Rb, Sr, Sm, Nd, Pb, and U concentrations for the three samples were measured by isotope dilution on the same solutions that were analyzed for isotopic compositions. An unsuccessful attempt was made to obtain a date on the Hole 900A rocks by $^{40}Ar/^{39}Ar$ analysis of a plagioclase separate consisting of relatively clean, but totally recrystallized plagioclase. The Sr, Nd, and Pb isotopes were analyzed at the Free University of Brussels isotope facility on a 7 collector VG sector mass spectrometer. The analytical procedure is entirely comparable to the one used for samples from the Ninetyeast Ridge on ODP Leg 121 (Weis and Frey, 1991). References for blank values and standard compositions (NBS Pb 981, Sr 987 and Nd Merck) can be found in Weis and Frey (1991). Mineral compositions were determined with the Iowa State University electron microprobe using well-analyzed mineral standards obtained from various sources.

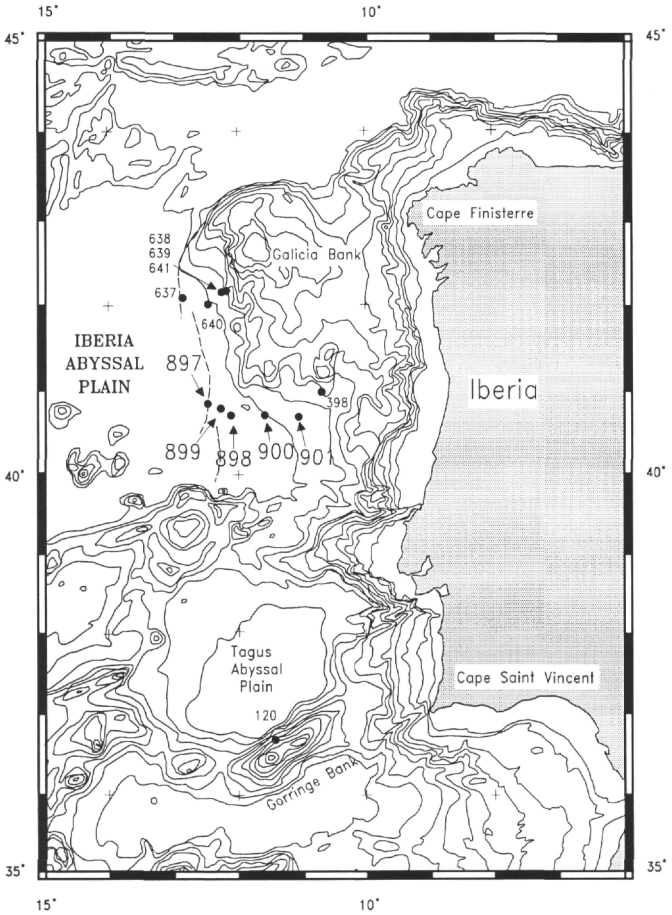

Figure 2. A map of the Iberia continental margin showing the location of the Leg 149 traverse and drill sites on the Iberia Abyssal Plain. Previous drill sites are also marked. The peridotite ridge drilled at Site 897, and earlier at Site 637, is marked with a dashed line. Modified from Sawyer, Whitmarsh, Klaus, et al. (1994).

DESCRIPTION OF THE METAMORPHOSED MAFIC ROCKS

Petrology

The Hole 900A metamorphosed mafic rocks consist of discontinuous bands of recrystallized plagioclase and clinopyroxene that surround large isolated porphyroclasts of strained plagioclase and clinopyroxene. The alternating discontinuous felsic and mafic bands define a poorly developed and highly variable characteristic foliation (Figs. 4-6). Shipboard core descriptions were difficult because the first samples were highly altered and green whereas later samples were fine-grained and gray with a poorly developed foliation. Thin section study showed that the foliation was caused by discontinuous bands of recrystallized plagioclase and clinopyroxene (Figs. 7A and B). A few large strained plagioclase and clinopyroxene porphyroclasts were observed within the finer grained recrystallized bands (Fig. 7C), revealing a coarse-grained precursor, although there is no way to know if the porphyroclasts represent primary minerals. Recrystallized bands are typically monomineralic (Fig. 7D), except for later alteration effects. X-ray diffraction (XRD) study indicated that even finer material in the mafic bands consists largely of amphibole. All of the Hole 900A mafic rocks are brecciated and veined by iron oxides, chlorite, epidote, clinozoisite, chalcedony, and lastly by calcite in places.

Our Hole 900A samples consist of between 40% and 70% plagioclase, with most of the remainder being clinopyroxene. All samples contain small amounts of retrograde minerals and some small veins. The composition of recrystallized plagioclase is typically labradorite between An_{53} and An_{67}, although it ranges from albite in more altered samples to calcic bytownite (Table 1). Adjacent bands of recrystallized plagioclase typically have similar compositions and reported microprobe compositions represent an average of 10 or more crystals from at least two different bands. Samples 149-900A-86R-1, 51-55 cm and 900A-82R-4, 64-69 cm contain unusually calcic plagioclase of An_{89} and An_{78} respectively, perhaps reflecting variations in the bulk composition of the magma from which primary crystals precipitated. Albite (An_6) occurs in Sample 149-900A-82R-3, 2-7 cm and sodic oligoclase (An_{11}) coexists with labradorite (An_{43}) in Sample 149-900A-81R-1, 96-101 cm, indicating local variations in retrograde metamorphism within the sample. The few plagioclase porphyroclasts analyzed are similar in composition to adjacent recrystallized calcic plagioclase, with the difference ranging from less than An_1 to almost An_9 in a sample where the plagioclases come from different parts of a thin section. No porphyroclasts were observed in the proximity of albite.

The only pyroxene observed in Hole 900A samples is clinopyroxene with a relatively constant composition ranging from En_{42} to En_{46}, Fs_6 to Fs_{13}, and Wo_{43} to Wo_{49} (Table 2). Recrystallized clinopyroxene in Sample 149-900A-86R-1, 51-55 cm, with the most calcic plagioclase (An_{89}), also has the highest Wo value (Wo_{49}). Two analyzed clinopyroxene porphyroclasts have compositions similar to adjacent recrystallized clinopyroxenes. The clinopyroxene retrogrades to fine-grained amphibole, chlorite and other minerals to varying degrees. We selected the least altered samples available; those with the least retrograded clinopyroxene, therefore less amphibole and other retrograde minerals, and core relatively free of veins.

Major Element Geochemistry

Major element ICP analyses of the Hole 900A metamorphosed mafic rocks confirms shipboard XRF analyses indicating that the original protolith of these rocks was either basalt or gabbro (Table 3). The variations in major element composition with depth in the core, calculated on an anhydrous basis, show some significant correlations (Fig. 8). The large TiO_2 and FeO_t peaks in Sample 149-900A-81R-1, 96-101 cm, correlate with the occurrence of opaque minerals; Core 149-900A-81R is the only part of the section in which opaque minerals were observed in thin section (Sawyer, Whitmarsh, Klaus, et al., 1994). Shipboard major and trace element data support such a limited occurrence for the opaque minerals (Gibson, et al., this volume). The Mg# is considerably lower in Sample 149-900A-81R-1, 96-101 cm, than in other samples because of the increase in FeO relative to MgO. One of the more obvious correlations, in samples other than the oxide sample and uppermost Sample 149-900A-80R-2, 107-112 cm, which is altered, is MgO with FeO_t and their anticorrelation with Al_2O_3 (Fig. 8). With the exception of Sample 149-900A-83R-3, 10-15 cm, Cr_2O_3 values correlate with FeO_t values as expected because Cr substitutes for trivalent Fe in clinopyroxene. In the lower part of the section, from Sample 149-900A-84R-3, 124-125 cm and below, there is a correlation between LOI and the oxidation index Fe_3/Fe_2 and an anticorrelation between LOI and MgO# suggesting that alteration is greatest where the Mg/Fe ratio is lowest. This is opposite to the pattern expected because rocks with a high Mg/Fe ratio should be further from equilibrium near the surface. In addition, there are mineralogically unexplained peaks in SiO_2 and Cr_2O_3, unexplained scatter in LOI, an unexplained anticorrelation between CaO and Fe_3/Fe_2, and gradual upward increases in Mg# that are not understood.

The abundance of Al_2O_3 correlates with plagioclase content better than CaO, as expected, because CaO content is influenced by small amounts of the Ca-rich secondary vein minerals calcite, epidote, and

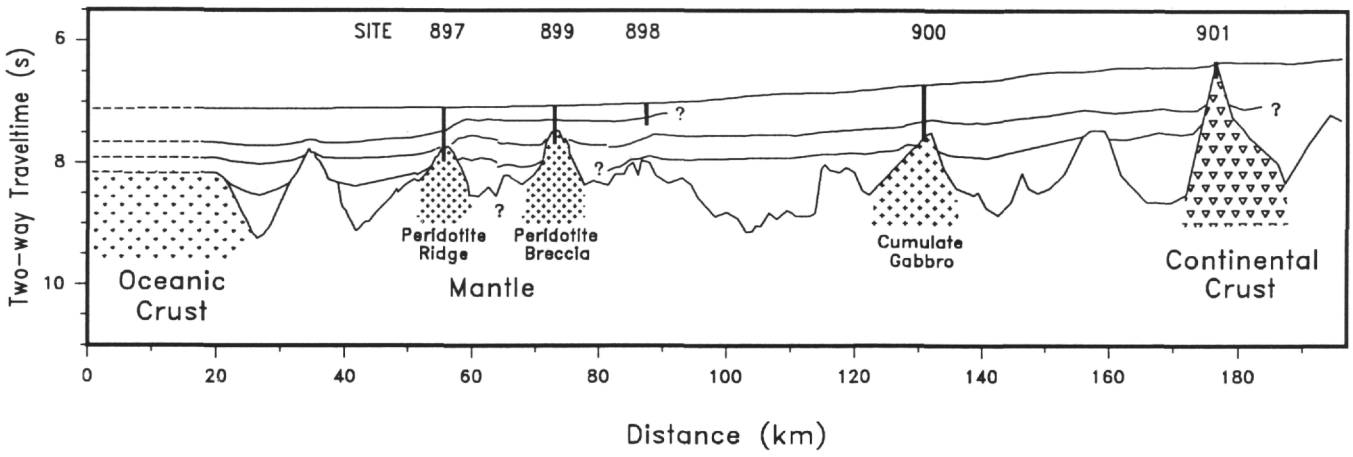

Figure 3. A roughly east-west geologic cross section across the Iberia Abyssal Plain showing the topography of the basement highs drilled on Leg 149 and shown on Figure 2. Vertical exaggeration is ×5. Modified from Sawyer, Whitmarsh, Klaus, et al. (1994).

clinozoisite. In addition, it is not clear what happens to Ca during albitization of labradorite; perhaps part of the Ca is captured by newly forming Ca-rich minerals while the remainder escapes from the immediate region by movement along vein fractures. In either case, the CaO will not correlate with the abundance of albitic plagioclase whereas most of the Al_2O_3 will remain within albite. The CaO peak in Sample 149-900A-82R-4, 64-69 cm, may, however, correlates with the calcic plagioclase (An_{78}) in that sample (Table 1). The anticorrelation between Al_2O_3 and MgO, FeO_t and Cr_2O_3 probably relates to the relative abundance of plagioclase versus clinopyroxene in these samples. The large Al_2O_3 peak in Sample 149-900A-84R-3, 124-125 cm, may be an extreme case of such variation since it correlates with low MgO, FeO_t, and Cr_2O_3 and a high abundance of plagioclase (70%) in thin section. The low value for SiO_2 in Sample 149-900A-86R-1, 51-55 cm, anticorrelates with Al_2O_3 and CaO, most likely reflecting the calcic nature of the plagioclase (An_{89}) in that sample (Table 1).

Trace Element Geochemistry

Incompatible trace element contents (Table 3) are low, which indicates that the protolith is a cumulate gabbro rather than a basalt or noncumulate (isotropic) gabbro. The chondrite-normalized rare earth element (REE) abundances are even closer to chondrite than N-MORB and, except for Sample 149-900A-81R-1, 96-101 cm with an N-MORB REE pattern, all samples have similar flat REE patterns near 2X-4X chondrite and positive europium (Eu) anomalies (Fig. 9). The positive Eu anomalies can be attributed to Eu in the cumulus plagioclase. The total range of REE values in the Hole 900A samples is small, La varies from 0.47 to 1.03, with all normalized values between 1X to 10X chondrite, and similar to cumulate gabbros from 26°N along the Mid-Atlantic Ridge (Tiezzi and Scott, 1980). However, Sample 149-900A-81R-1, 96-101 cm has a REE pattern distinct from the other Hole 900A metamorphosed mafics with heavy rare earth element (HREE) values near 10X chondrite and a strong light rare earth element (LREE) depletion (Fig. 9). Its REE pattern is similar to N-MORB basalts from normal segments of the Mid-Atlantic Ridge (Schilling et al., 1983), which indicates retention of considerably more magma than the typical Hole 900A cumulate gabbro and suggests a MORB parental magma.

The typical Hole 900A metamorphosed mafic rock spider diagram (Fig. 10) supports the REE plot analysis indicating a cumulate origin. Furthermore the spider diagram suggests that the large ion lithophile elements (LILE) K, Rb, Ba, and Sr have been enriched by hydrous solutions. The LILE, REE, and high field strength elements (HFSE) represent incompatible element groups that travel together in magma and should be expected to increase or decrease together producing smooth spider diagram patterns (Fig. 11). If the LILE have a greater or lesser abundance than the other incompatible element groups, hydrous solutions are most likely the transporting medium, rather than magma, because the LILE are far more soluble in hydrous fluids than the REE and HFSE. Spider diagrams include some of all three incompatible element groups. The less mobile REE and HFSE in the Hole 900A rocks have an abundance lower than that of any basalt, even N-MORB, but typical of cumulate gabbros from 26°N on the Mid-Atlantic Ridge (Tiezzi and Scott, 1980). The low abundance of the less mobile elements contrasts with the high abundance of the more mobile LILE which have anomalously high peaks on the typical Hole 900A spider diagram (Fig. 10). The elements which appear to be enriched on the spider diagram are K, Rb, Ba, Sr, U, and to a lesser extent Eu, although the K, Sr, and Eu peaks are probably enlarged because of the plagioclase-rich nature of these cumulates. The relatively low abundance of the immobile REE and HFSE indicates that little magma was retained by the Hole 900A cumulate gabbros.

Isotopic Geochemistry

Three large powdered samples were prepared for isotopic analysis by combining the smaller Samples 149-900A-81R-1, 96-101 cm and 900A-81R-2, 82-87 cm into Sample 81, Samples 149-900A-82R-1, 128-134 cm and 900A-82R-2, 106-111 cm into Sample 82, and Samples 149-900A-85R-1, 26-30 cm and 900A-85R-5, 51-56 cm into Sample 85. The Sr, Nd, and Pb isotopic ratios and Rb, Sr, Sm, Nd, Pb, and U elemental concentrations for these three Hole 900A metamorphosed mafic rocks are given in Table 4. All of the Nd and Pb isotopic ratios, except $^{207}Pb/^{204}Pb$, fall within oceanic fields similar to MORB. The Sr isotopic ratios are far too high and reflect seawater alteration (Figs. 12, 13). The generally high and variable U/Pb ratio, 0.10 to 0.81, and the generally low and variable Th/U ratio, 0.02 to 1.0, of the Hole 900A mafic rocks indicate secondary addition of highly soluble U from seawater (Michard and Albarede, 1985; Chen et al., 1986). This enrichment of U was revealed previously by the typical Hole 900A spider diagram (Fig. 10).

Our attempt to date the Hole 900A metamorphic mafic rocks by $^{40}Ar/^{39}Ar$ was unsuccessful, but an $^{40}Ar/^{39}Ar$ age of 136.4 Ma has been obtained by Feraud et al. (this volume). Consequently all isotopic ratios have been corrected for in situ decay of ^{87}Rb, ^{147}Sm, ^{235}U, and ^{238}U using that age value for Hole 900A rocks. The relatively high $^{143}Nd/^{144}Nd$ ratios correspond to initial positive ϵ_{Nd} values greater than six at 136.4 Ma, which indicate a MORB source (Fig. 12). The

Figure 4. Typical foliation bands in the metamorphosed mafic rocks are discontinuous and fine, often being displaced and reoriented at fractures and veins, as observed in Sample 149-900A-82R-1, 100-111 cm. The foliation trend is variable and locally curved near fractures in a manner similar to drag folding.

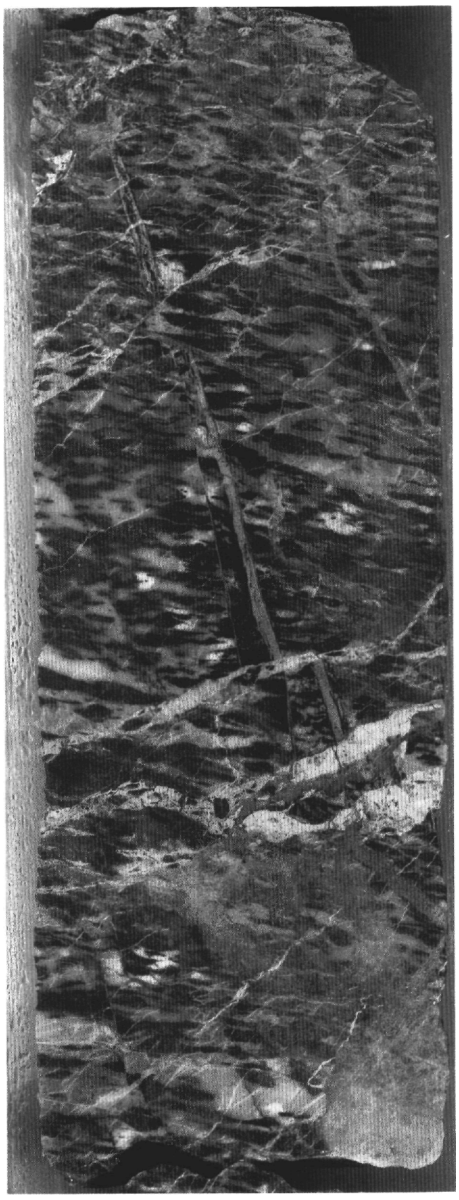

Figure 5. Local foliation in the metamorphosed mafic rocks is coarse and variable in width within individual bands as observed in Sample 149-900A-82R-5, 13-29 cm. The foliation is cut by several generations of veins and displacement of one set by another is shown near the center of the photograph. Some of the veins contain broken fragments of the foliated metamorphosed mafic rock.

initial lead isotope ratios appear to allow an OIB origin, but have been displaced because of seawater alteration (Fig. 13). The large correction required for in situ decay for the Hole 900A rocks is caused by high μ (Tatsumoto, 1978) for these rocks. Both the higher $^{87}Sr/^{86}Sr$ ratios (>.7045) and the high $^{238}U/^{204}Pb$ ratios (29.7 to 69.4) indicate seawater alteration. Alteration of the Sr isotopics without significant resetting of the Nd isotopics limits the water/rock ratio during seawater alteration to less than 10^8, and suggests a value closer to 10^5 (McCulloch et al., 1980). The $^{18}O/^{16}O$ composition of the three Hole 900A samples lie between 4.22 and 3.48 per mil, while the typical magmatic values are at 5.5 per mil; again, this clearly reflects seafloor alteration.

DISCUSSION

Secondary Features

The most conspicuous feature of the Hole 900A rocks is the poorly developed and discontinuous foliation (Figs. 4-6) of recrystallized plagioclase and clinopyroxene. This foliation is typical of high-temperature metamorphism near ridges on the ocean floor, but is not typical of foliation produced by continental orogeny in high-grade metamorphic rocks. Indian Ocean gabbros recovered from Hole 735B on the Atlantis II Fracture Zone metamorphosed to granulite-facies temperatures display deformational and compositional features (Cannat, 1991) similar to those at Hole 900A. These features appear to be

characteristic of metamorphosed cumulate gabbros from slow-spreading ridges (Mével and Cannat, 1991). Approximately 30% of the 435 m of Hole 735B gabbros recovered are plastically deformed and recrystallized to amphibolite- and granulite-facies temperatures, compared to 100% of the 27.7 m of metamorphosed mafic rock recovered at Hole 900A, allowing preservation of primary minerals and textures in the Hole 735B rocks. Metamorphosed Hole 735B gabbros contain areas with coarsely recrystallized plagioclase, clinopyroxene, olivine, orthopyroxene, oxides, and apatite, a mineral assemblage that would be considered indicative of granulite-facies continental metamorphism (Yardley, 1989). The Hole 900A rocks consist largely of bands of medium- to fine-grained recrystallized plagioclase and bands of clinopyroxene partially retrograded to fine-grained amphibole that often is identified from XRD powder patterns. The formation of amphibole from the anhydrous plagioclase-clinopyroxene assemblage requires the addition of hydrous fluids.

The Hole 900A rocks have gained K_2O and other LILE plus U, while other major oxides and trace elements appear to have remained unchanged. The Hole 900A metamorphosed mafics have major element compositions similar to cumulate gabbros from a variety of sources (Gunn and Roobol, 1977; Tiezzi and Scott, 1980; Meyer et al., 1989) in all respects except for high LILE and U. The average K_2O content in the Hole 900A rocks is about 20 times higher than that of a typical cumulate gabbro. Experimental studies of the alteration patterns produced in mafic rocks by seawater at temperatures of 500°C and below (Hajash, 1975; Humphris and Thompson, 1978; Mottl and Holland, 1978; Seyfried and Bischoff, 1979; Hajash and Archer, 1980) indicate that, in addition to a gain or loss of K_2O, MgO is consistently gained and CaO is consistently lost. A gain of K_2O, such as in the Hole 899B basalt and diabase clasts (Seifert and Brunotte, chapter 29, this volume), combined with the gain of MgO and loss of CaO, is regarded as indicative of seafloor weathering at temperatures below 200°C (Seyfried and Bischoff, 1978). At temperatures above 200°C and up to at least 500°C, experimental studies found that K_2O is lost. However, hydration of the Hole 735B gabbros was typically accompanied by increases in CO_2, ferric iron, and K_2O (Robinson et al., 1991).

The addition of K, and probably the other LILE and U, appears to have occurred during hydration and retrograde metamorphism of the Hole 900A mafic rocks. Only approximately one-quarter of the K_2O in the Hole 900A rocks resides in the structure of the abundant metamorphic recrystallized plagioclase, with up to 0.48% K_2O (Table 1). The other three-quarters of the K_2O is concentrated in small scattered patches of alteration within plagioclase porphyroclasts (Fig. 14) and along grain boundaries between recrystallized plagioclase and clinopyroxene (Fig. 15). The soft K_2O-rich alteration patches are marked by small irregular pits on the surface of polished microprobe sections that make accurate analysis difficult. Nevertheless, it appears that K_2O concentrations reach at least 15% locally. The association of K with fibrous amphibole in alteration patches (Fig. 14) would seem to indicate it was introduced by hydrous solutions during the retrograde metamorphism. The brown iron stain typical of many alteration patches may indicate the event was also one of increased oxidation.

Primary Composition

Cumulate gabbros should be expected to have low K_2O, P_2O_5, TiO_2, and incompatible trace element contents because these elements are not incorporated within the structures of early cumulus minerals from basaltic magma. Cumulate and noncumulate (or isotropic) gabbros, that are similar in mineralogy and major element geochemistry, can typically be distinguished by differences in incompatible trace element abundances. Noncumulate or isotropic gabbros are compositionally equivalent to basalts in that they represent solidified magma and have trace element abundances similar to basalts. Cumulate gabbros, with mineralogies and major element compositions similar to isotropic gabbros, consist of minerals that have separated from all or part of the magma from which they crystallized. Consequently, they have lost the majority of incompatible elements, which stay in the magma. Consequently, the incompatible element content of a cumulate rock depends largely on the amount of magma that has been trapped between accumulating crystals, plus some small amount within the cumulus minerals. An example of the difference between related isotropic and cumulate gabbros was illustrated by Leterrier (1985) and has been observed in many other regions. The difference in incompatible element content is often especially obvious on a REE diagram, with isotropic gabbro having a REE abundance near 10X chondrite or above, similar to basalt, whereas cumulate gabbro typically has a REE abundance between 1X-5X chondrite. The lack of incompatible elements is typical of cumulate rocks, as well as rocks from which magma has been removed by partial melting, because, by definition, these elements travel with the magma.

Figure 6. The discontinuous nature of foliation bands and their abrupt width changes over short distances is illustrated near the center of Sample 149-900A-82R-1, 74-88 cm.

As a result, cumulate gabbros from all tectonic provinces have similar elemental compositions because the incompatible elements

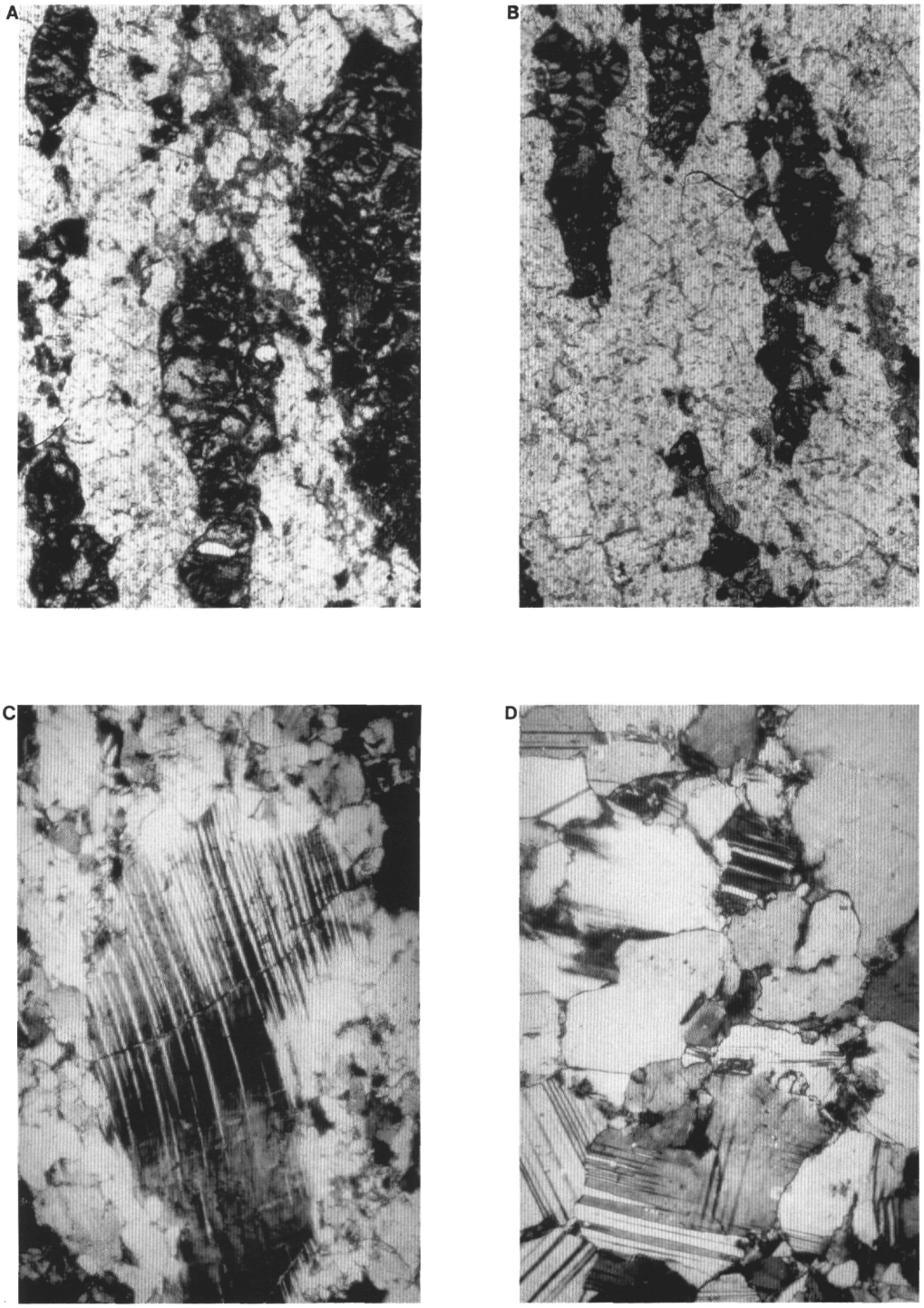

Figure 7. Photomicrographs of the Hole 900A metamorphosed mafic rocks. **A.** Discontinuous oriented bands of recrystallized plagioclase crystals (light) and recrystallized clinopyroxene crystals (dark) in Sample 149-900A-86R-1, 51-55 cm, in plane-polarized light (PPL), that define the foliation observed in Figures 4-6. The wide dimension of the photomicrograph = ~2.7 mm. **B.** Another photomicrograph of the discontinuous oriented plagioclase and clinopyroxene bands in Sample 149-900A-83R-1, 0-6 cm, in PPL showing thin alteration rims around individual recrystallized plagioclase crystals. Typically, the alteration rims appear to be chlorite. The wide dimension of the photomicrograph = ~2.7 mm. **C.** A large strained and twinned plagioclase porphyroclast surrounded by smaller unstrained recrystallized plagioclase crystals in one of the discontinuous oriented plagioclase bands from Sample 149-900A-83R-2, 67-70 cm, in cross-polarized light (XPL). The wide dimension of this photomicrograph is ~0.7 mm. **D.** A patch of more coarsely recrystallized plagioclase within a plagioclase band from Sample 149-84R-4, 72-76 cm, in XPL showing the abundant twinning and altered crystal boundary regions sometimes observed in the plagioclase bands. The wide dimension of this photomicrograph is ~0.7 mm.

Table 1. Plagioclase composition in Hole 900A metamorphosed cumulate gabbros.

	80R-1*, 21–22	80R-1*, 21–22	80R-2, 107–112	81R-1, 96–101	81R-1, 96–101	81R-2*, 82–87	82R-1, 101–106	82R-1, 128–134	82R-3, 2–7	82R-4, 64–69	83R-1, 0–6	83R-2, 60–65
	recrystall	porphyro	recrystall	recrystall	recrystall	recrystall	recrystall	recrystall	recrystall	recrystall	recrystall	recrystall
Major oxides (wt%)												
SiO_2	50.69	52.55	50.40	65.11	56.25	54.13	52.79	51.49	66.35	47.34	51.83	50.58
Al_2O_3	31.47	30.02	31.98	21.98	27.75	28.99	30.67	31.62	20.79	34.39	30.20	31.48
FeOt	0.10	0.08	0.06	0.04	0.14	0.22	0.08	0.09	0.04	0.05	0.08	0.05
MgO	0.17	0.17	0.10	0.03	0.12	0.18	0.15	0.11	0.07	0.13	0.12	0.24
CaO	14.09	12.25	13.94	2.31	8.74	10.97	12.03	13.45	1.30	15.59	12.63	12.87
SrO	—	—	0.13	0.12	0.18	0.10	0.16	0.14	0.08	0.15	0.09	0.10
BaO	—	—	0.02	0.04	0.08	0.01	—	—	0.01	0.06	0.01	0.07
Na_2O	3.46	4.34	3.53	10.37	6.18	5.07	4.40	3.95	11.01	2.23	4.49	3.98
K_2O	0.31	0.48	0.20	0.06	0.24	0.34	0.18	0.12	0.01	0.35	0.10	0.10
Total	100.29	99.89	100.36	100.06	99.68	100.01	100.46	100.97	99.66	100.29	99.55	99.47
%An	68.05	59.27	67.81	10.95	43.24	54.86	59.59	64.88	6.12	77.78	60.54	63.76
%Ab	30.15	37.98	31.03	88.74	55.31	44.63	39.33	34.45	93.82	20.10	38.89	35.62
%Or	1.80	2.75	1.17	0.31	1.45	0.51	1.08	0.66	0.07	2.12	0.58	0.62

	83R-2, 60–65	83R-2*, 67-70	83R-3, 10-15	84R-4*, 72-76	84R-4*, 72-76	85R-1, 30-36	85R-2, 2-7	85R-5*, 51-56	85R-5*, 51-56	85R-5, 88-93	86R-1, 51-55
	porphyro	recrystall	recrystall	recrystall	porphyro	recrystall	recrystall	recrystall	porphyro	recrystall	recrystall
Major oxides (wt%)											
SiO_2	51.58	53.74	53.35	52.65	52.80	52.84	50.42	51.29	50.91	51.27	45.08
Al_2O_3	30.90	28.79	30.22	30.04	29.65	29.58	31.71	31.50	31.98	31.01	35.45
FeOt	0.05	0.13	0.10	0.17	0.14	0.07	0.07	0.12	0.09	0.10	0.03
MgO	0.22	0.15	0.07	0.16	0.16	0.19	0.22	0.23	0.24	0.21	0.24
CaO	12.79	12.01	11.65	12.30	12.37	11.53	13.50	13.49	13.39	12.91	18.08
SrO	0.10	—	0.13	—	—	0.17	0.10	0.10	0.11	0.10	0.15
BaO	0.04	—	—	—	—	—	0.01	0.02	0.01	0.02	0.03
Na_2O	3.87	4.85	4.88	4.72	4.61	4.68	3.61	3.64	3.79	4.10	1.28
K_2O	0.10	0.15	0.24	0.12	0.12	0.22	0.08	0.15	0.15	0.14	0.02
Total	99.65	99.82	100.64	100.16	99.85	99.28	99.72	100.54	100.67	99.86	100.36
%An	64.26	57.31	56.14	58.66	59.36	56.94	67.06	66.62	65.59	63.01	88.57
%Ab	35.12	41.82	42.49	40.64	39.96	41.77	32.43	32.50	33.57	36.15	11.29
%Or	0.62	0.87	1.37	0.70	0.68	1.28	0.50	0.88	0.85	0.84	0.14

Note: No good plagioclase analyses were obtained for Samples 82R-2, 106-111 cm; 84R-3, 124-129 cm; 84R-4, 123-126 cm, and 85R-1, 26-30 cm. * = thin sections only; no bulk chemical data are available for these samples. Recrystall = recrystallized, porphyro = porphyroclast, An = normative anorthite, Ab = normative albite, Or = normative orthoclase.

Table 2. Clinopyroxene composition in Hole 900A metamorphosed cumulate gabbros.

	80R-2, 107–112	80R-2, 107–112	82R-1, 128–134	83R-1, 0–6	85R-1, 2–7	85R-1, 30–36	85R-5, 51–56	86R-1, 51–55
	recrystall	porphyro	porphyro	recrystall	recrystall	recrystall	recrystall	recrystall
Major oxides (wt%)								
SiO_2	51.26	51.02	51.35	50.11	49.98	52.24	50.29	53.51
TiO_2	0.51	0.46	0.42	0.65	0.67	0.52	0.78	0.04
Al_2O_3	4.31	5.17	3.75	5.39	5.61	5.32	5.38	0.94
FeOt	5.06	4.11	6.75	7.22	7.67	6.28	6.94	3.93
MnO	0.15	0.13	0.20	0.20	0.20	0.15	0.20	0.05
MgO	15.51	15.71	14.39	14.00	14.13	14.73	14.21	16.26
CaO	22.41	22.14	22.50	21.37	20.11	19.55	21.33	25.02
Na_2O	0.65	0.68	0.55	0.79	0.74	0.77	0.73	0.15
K_2O	0.01	0.00	0.01	0.05	0.03	0.02	0.01	0.03
Total	99.87	99.42	99.92	99.78	99.14	99.58	99.87	99.93
%En	44.90	46.20	41.76	41.77	42.82	45.48	42.37	44.58
%Fs	8.46	7.00	11.32	12.41	13.38	11.13	11.93	6.12
%Wo	46.64	46.81	46.92	45.82	43.80	43.39	45.70	49.30

Note: recrystall = recrystallized, porphyro = porphyroclast, En = normative enstatite, Fs = normative ferrosilite, Wo = normative wollastonite.

used to distinguish between basaltic magmas from different sources (see Seifert and Brunotte, chapter 29, this volume) are largely lost with the escaping magma. Cumulate gabbros formed at mid-ocean ridges have elemental compositions similar to the cumulate gabbros at Hole 900A (Thompson, 1973; Engel and Fisher, 1975; Tiezzi and Scott, 1980; Miyashiro and Shido, 1980; Meyer et al., 1989; Hekinian et al., 1993), as do cumulate gabbros from other tectonic provinces. Cumulate gabbros can be either oceanic, those formed at a divergent ridge, back-arc basin, or even an island arc (Gerlach et al., 1981; Beard, 1986), or continental, those associated with a layered igneous complex. Ophiolitic cumulate gabbros are believed to have formed in all of the distinct oceanic tectonic provinces, although most may represent back-arc basins (Serri, 1981). Only isotopic data allow a distinction to be made between the various tectonic provinces in the oceans and continents (Coish et al., 1982).

On an AFM diagram the Hole 900A metamorphosed gabbroic rocks plot below the Skaergaard trend and N-MORB but with cumulate gabbros from a variety of tectonic provinces (Fig. 16). Part of the scatter is related to differences in the mineralogy of different cumulate gabbros, part relates to the amount of trapped magma, and part may be caused by later alteration. A lack of oxide minerals in all parts of the Hole 900A rocks, except Core 900A-81R which plots next to N-MORB as expected, offers mineralogical evidence for a cumulate origin for most of these rocks. Note that one of the ophiolitic cumulate gabbros also plots near N-MORB and would also be expected to have retained considerable trapped magma. The wide variation in plagioclase composition (An_{43} to An_{89}) in the Hole 900A rocks, ignoring the retrograde albite, suggests compositional differences, in the magma from which primary plagioclase precipitated, that are probably best explained by multiple magma injections.

No textural information remains to determine if the large strained porphyroclasts represent primary igneous minerals or a previous generation of metamorphic minerals. The Hole 900A samples are characterized by discontinuous foliation bands of recrystallized plagioclase and clinopyroxene containing large isolated strained porphyroclasts of plagioclase (Fig. 7C) or clinopyroxene, respectively. Because of their large size, it seems likely that the porphyroclasts represent relicts of the primary igneous mineralogy that have survived the later metamorphism. The similar composition of recrystallized clinopyroxene and plagioclase and adjacent porphyroclasts, from which the recrystallized minerals were probably derived, suggests recrystallization in a closed system with only two phases involved. Alternatively, the porphyroclasts were compositionally re-equilibrated with recrystallizing minerals during the recrystallization event without being totally destroyed or recrystallized. If the first explanation is correct, the trace element composition of the parental magma can be estimated from the appropriate partition coefficients.

Parental Magma Composition

The trace element composition of the parental magma can be estimated from the bulk trace element composition of a cumulate rock using the appropriate mineral partition coefficients assuming certain conditions are met. First, it must be assumed that little or no trapped magma is present so that most of the incompatible elements reside in the cumulus minerals. The depletion of the more immobile incompatible trace elements indicates this to be the case for all parts of the Hole 900A section except Core 900A-81R. Second, as mentioned above, it has to be assumed that, to a first approximation, the Hole 900A cumulate gabbros primary mineralogy was dominated by plagioclase and clinopyroxene with all other minerals being minor. No relicts of olivine or orthopyroxene have been found and opaque minerals are confined to Core 900A-81R. On the basis of these assumptions, the trace element composition of the parental magma can be estimated from literature partition coefficients for plagioclase and clinopyroxene (Drake and Weill, 1975; Arth, 1976; Baitis and Lindstrom, 1980; Henderson, 1982; Rollinson, 1993). When this exercise is carried out for the seven REEs for which instrumental neutron activation analysis has provided good mineral separate data, and thus good partition coefficients, a nearly flat chondrite normalized REE pattern is obtained that resembles transitional MORB (Fig. 17). The transitional MORB pattern is obtained from average values taken from all Hole 900A samples except Sample 149-900A-81R-1, 96-101 cm; this sample was omitted because of its distinct mineralogy and relatively enriched trace element composition. A transitional MORB parental magma for these cumulate gabbros would be consistent with the environment in which these rocks have been found, and agrees with our isotopic data indicating a MORB origin.

CONCLUSIONS

The Hole 900A rocks exhibit compositional and textural characteristics of cumulate gabbros formed, metamorphosed, and enriched by seawater alteration at or near a mid-ocean ridge. The major element composition of these rocks is typical of basalt or gabbro enriched in LILE by later seawater interaction. The depleted trace element composition is typical of cumulate gabbros that have lost essentially all of the trapped magma before solidification. Nd isotopic data indicate the cumulate gabbros have a MORB origin and have been enriched in U and Sr from seawater. The metamorphic style, with discontinuous bands of recrystallized plagioclase and pyroxene and incomplete destruction of porphyroclasts, is similar to Hole 735B metamorphosed gabbros. It is also probably typical of high-grade seafloor metamorphism and very atypical of high-grade continental

Table 3. Major and trace element composition of Hole 900A metamorphosed cumulate gabbros.

	80R-2, 107–112	81R-1, 96–101	82R-1, 101–106	82R-1, 128–134	82R-3, 2–7	82R-4, 64–69	83R-1, 0–6	83R-2, 60–65	83R-3, 10–15	84R-3, 124–129	84R-4, 123–126	85R-1, 26–30	85R-1, 30–36	85R-2, 2–7	85R-5 88–93	86R-1, 51–55	Ave900A Gabbro
Major oxides (wt%)																	
SiO_2	45.52	45.45	44.31	46.90	44.00	47.93	49.91	47.26	45.12	46.90	45.70	46.86	45.46	46.38	45.86	44.83	46.15
TiO_2	0.14	1.20	0.27	0.21	0.24	0.24	0.23	0.42	0.18	0.14	0.28	0.28	0.29	0.24	0.34	0.37	0.32
Al_2O_3	19.92	17.18	17.69	20.61	15.54	18.22	18.92	16.19	17.68	22.69	15.11	16.38	13.32	18.98	16.75	18.60	17.74
Cr_2O_3	0.07	0.04	0.08	0.06	0.06	0.07	0.06	0.13	0.03	0.02	0.15	0.11	0.13	0.07	0.09	0.08	0.08
Fe_2O_3	1 .28	1.91	1.33	0.83	1.03	1.14	2.14	1.55	3.38	1.34	0.83	1.06	1.31	0.90	2.33	1.21	1.47
FeO	3.11	8.30	3.34	4.35	5.82	3.92	2.64	4.63	5.56	3.72	5.57	5.16	5.96	4.00	3.94	2.84	4.55
MnO	0.09	0.17	0.09	0.06	0.10	0.07	0.09	0.11	0.13	0.06	0.12	0.11	0.13	0.09	0.10	0.05	0.10
MgO	11.68	9.07	9.08	9.89	12.75	8.54	8.08	8.77	11.62	6.45	12.05	11.13	13.14	7.64	11.06	10.57	10.10
CaO	7.46	8.15	12.98	9.69	8.17	12.36	9.45	13.97	6.94	9.98	13.80	13.16	13.95	14.35	11.95	15.44	11.36
Na_2O	2.45	2.41	2.05	2.19	2.96	1.49	3.33	1.93	1.72	2.61	1.60	1.84	1.25	2.17	2.09	0.70	2.05
K_2O	0.84	0.58	1.13	0.54	0.62	0.72	0.59	0.41	0.92	0.89	0.32	0.36	<.05	0.39	0.25	0.49	0.57
P_2O_5	0.02	0.01	<.01	0.01	0.01	0.02	0.01	0.02	<.01	<.01	0.02	0.03	0.01	0.03	0.02	0.01	0.01
LOI	7.00	4.50	7.20	3.80	8.00	4.50	4.00	4.00	5.60	4.00	3.40	2.50	4.00	3.80	4.50	4.00	4.68
Total	99.58	98.97	99.55	99.14	99.30	99.22	99.45	99.39	98.88	98.80	98.95	98.98	98.95	99.04	99.28	99.19	99.17
FeOt	4.26	10.02	4.54	5.09	6.75	4.95	4.57	6.03	8.60	4.92	6.32	6.11	7.14	4.82	6.04	3.93	5.88
Fe_3/Fe_2	0.41	0.23	0.40	0.19	0.18	0.29	0.81	0.33	0.61	0.36	0.15	0.21	0.22	0.23	0.59	0.43	0.35
Mg#	85	66	81	80	80	78	79	75	74	73	80	79	79	77	79	85	78.13
Trace elements (ppm)																	
La	0.56	0.47	0.78	0.80	0.73	0.75	0.87	1.03	0.72	0.75	0.91	0.88	0.76	0.87	0.96	0.93	0.80
Ce	1.09	1.12	1.36	1.50	1.58	1.52	1.85	2.25	1.39	1.35	1.99	1.82	1.66	1.70	2.18	2.05	1.65
Pr	0.21	0.28	0.27	0.26	0.29	0.30	0.33	0.42	0.23	0.22	0.37	0.34	0.36	0.32	0.40	0.41	0.31
Nd	1.03	2.01	1.31	1.27	1.50	1.50	1.70	2.31	1.12	0.94	1.99	1.84	1.96	1.63	2.19	2.25	1.66
Sm	0.41	1.16	0.59	0.51	0.62	0.62	0.70	1.03	0.43	0.32	0.85	0.78	0.81	0.68	0.92	0.97	0.71
Eu	0.29	0.66	0.30	0.33	0.26	0.32	0.54	0.60	0.41	0.33	0.46	0.47	0.43	0.46	0.56	0.33	0.42
Gd	0.66	1.77	0.83	0.68	0.82	0.85	0.94	1.37	0.56	0.42	1.11	0.98	1.14	0.85	1.18	1.30	0.97
Tb	0.12	0.37	0.17	0.13	0.17	0.17	0.19	0.28	0.11	0.08	0.23	0.20	0.24	0.17	0.24	0.27	0.20
Dy	0.77	2.45	1.10	0.85	1.09	1.05	1.18	1.82	0.70	0.46	1.46	1.38	1.56	1.13	1.57	1.75	1.27
Ho	0.16	0.52	0.23	0.17	0.22	0.21	0.24	0.38	0.15	0.10	0.31	0.28	0.31	0.23	0.33	0.37	0.26
Er	0.45	1.56	0.63	0.48	0.63	0.60	0.67	1.07	0.41	0.26	0.85	0.81	0.86	0.64	0.94	1.05	0.74
Tm	0.06	0.21	0.08	0.06	0.09	0.08	0.09	0.14	0.06	0.03	0.11	0.10	0.12	0.08	0.12	0.14	0.10
Yb	0.37	1.34	0.51	0.38	0.51	0.49	0.55	0.83	0.34	0.21	0.68	0.62	0.70	0.51	0.75	0.84	0.60
Lu	0.06	0.20	0.08	0.06	0.08	0.08	0.09	0.13	0.05	0.03	0.11	0.10	0.11	0.08	0.12	0.13	0.09
Y	3.85	12.69	5.50	4.18	5.49	5.49	6.01	9.35	3.65	2.47	7.75	7.17	7.84	5.97	8.48	9.86	6.61
Nb	0.23	0.07	0.20	0.22	0.17	0.17	0.13	0.35	0.15	0.20	0.22	0.19	0.21	0.18	0.28	0.20	0.20
Ta	0.02	0.01	0.01	0.02	0.01	0.02	0.01	0.02	0.01	0.01	0.02	0.02	0.02	0.01	0.02	0.01	0.02
Hf	0.19	0.56	0.24	0.21	0.24	0.22	0.24	0.49	0.17	0.12	0.34	0.32	0.34	0.26	0.41	0.38	0.30
Th	0.03	0.01	0.09	0.02	0.02	0.01	0.01	0.03	0.02	0.03	0.02	0.02	0.02	0.01	0.02	0.01	0.02
U	0.05	0.46	0.30	0.07	0.22	0.08	0.08	0.15	0.20	0.10	0.04	0.08	0.02	0.05	0.09	0.05	0.13
Pb	0.26	0.76	0.37	0.59	0.53	0.19	0.36	0.30	0.72	0.41	0.24	0.27	0.21	0.23	0.38	0.12	0.37
Ba	183	116	121	76	50	129	85	68	68	82	42	43	24	61	46	48	77.6
Rb	6.09	4.64	9.05	4.79	5.65	7.96	6.73	5.55	10.37	9.49	1.69	2.35	1.25	3.89	2.39	5.26	5.45
Cs	0.06	0.03	0.06	0.04	0.04	0.14	0.06	0.11	0.23	0.18	0.07	0.05	0.04	0.05	0.03	0.07	0.08
Sr	320	209	261	297	279	424	322	212	233	320	186	239	191	282	259	360	275
Ni	184	80	107	157	168	126	84	107	220	125	173	176	202	106	155	123	143
Co	38	54	33	43	57	36	31	34	59	42	45	43	51	33	39	33	41.9
Sc	23	48	41	31	34	37	37	56	24	15	47	44	48	38	44	55	38.9
Zn	31	65	19	19	22	19	19	26	57	18	22	30	37	21	30	18	28.3

Note: Mg# based on FeO = 0.85 FeO_t

metamorphism. A loosely constrained parental magma calculation yields a REE pattern similar to transitional MORB. Our data and the $^{40}Ar/^{39}Ar$ age of 136.4 Ma by Feraud et al. (this volume) are consistent with the conclusion that the Hole 900A rocks were formed and synchronously metamorphosed at or near the present site as the Atlantic Ocean started to open.

ACKNOWLEDGMENTS

The first author appreciates the opportunity to have been a shipboard petrologist on Leg 149, the guidance and patience of Co-Chief scientists Dale Sawyer and Bob Whitmarsh, and the support of an excellent technical staff and facilities on the ship. Data gathering for this study was supported by USSSP Grant# 0040 to the first author. This manuscript has been greatly improved by the constructive reviews of Tracy Vallier and Michael Mottl as well as the comments of the ODP editorial staff. The authors are especially grateful to GeoAnalytical Laboratory analyst Charles Knaap for his careful ICP/MS analyses of these rocks. We would also like to thank Jean-Paul Mennessier for his assistance with the isotope geochemistry.

REFERENCES

Anders, E., and Grevesse, N., 1989. Abundances of the elements: meteoritic and solar. *Geochim. Cosmochim. Acta,* 53:197-214.

Arth, J.G., 1976. Behaviour of trace elements during magmatic processes: a summary of theoretical models and their applications. *J. Res. U.S. Geol. Surv.,* 4:41-47.

Baitis, H.W., and Lindstrom, M.M., 1980. Geology, petrography, and petrology of Pinzon Island, Galapagos Archipelago. *Contrib. Mineral. Petrol.,* 72:367-386.

Beard, J.S., 1986. Characteristic mineralogy of arc-related cumulate gabbros: implications for the tectonic setting of gabbroic plutons and for andesite genesis. *Geology,* 14:848-851.

Beccaluva, L., Ohnenstetter, D., Ohnenstetter, M., and Venturelli, G., 1977. The trace element geochemistry of Corsican ophiolites. *Contrib. Mineral. Petrol.,* 64:11-31.

Beslier, M.-O., Ask, M., and Boillot, G., 1993. Ocean-continent boundary in the Iberia Abyssal Plain from multichannel seismic data. *Tectonophysics,* 218:383-393.

Boillot, G., Winterer, E.L., Meyer, A.W., et al., 1987. *Proc. ODP, Init. Repts.,* 103: College Station, TX (Ocean Drilling Program).

Cannat, M., 1991. Plastic deformation at an oceanic spreading ridge: a microstructural study of Site 735 gabbros (southwest Indian Ocean). *In* Von Herzen, R.P., Robinson, P.T., et al., *Proc. ODP, Sci. Results,* 118: College Station, TX (Ocean Drilling Program), 399-408.

Chen, J.H., Wasserburg, G.J., von Damm, K.L., and Edmond, J.M., 1986. The U-Th-Pb systematics in hot springs on the East Pacific Rise at 21°N and Guaymas Basin. *Geochim. Cosmochim. Acta,* 50:2467-2479.

Cohen, R.S., and O'Nions, R.K., 1982. Identification of recycled continental material in the mantle from Sr, Nd and Pb investigations. *Earth Planet. Sci. Lett.,* 61:73-84.

Coish, R.A., Hickey, R.L., and Frey, F.A., 1982. Rare earth element geochemistry of the Betts Cove ophiolite, Newfoundland. *Geochim. Cosmochim. Acta.,* 46:2117-2134.

Davies, G.R., Norry, M.J., Gerlach, D.C., and Cliff, R.A., 1989. A combined chemical and Pb-Sr-Nd isotope study of the Azores and Cape Verde hotspots: the geodynamic implications. *In* Saunders, A.D., and Norry, M.J. (Eds.), *Magmatism in the Ocean Basins.* Geol. Soc. Spec. Publ. London, 42:231-255.

Dosso, L., Bougault, H., and Joron, J.L., 1993. Geochemical morphology of the North Atlantic Ridge, 10°-24°N: trace element-isotope complementarity. *Earth Planet. Sci. Lett.,* 120:443-462.

Drake, M.J., and Weill, D.F., 1975. Partition of Sr, Ba, Ca, Y, Eu^{2+}, Eu^{3+}, and other REE between plagioclase feldspar and magmatic liquid: an experimental study. *Geochim. Cosmochim. Acta,* 39:689-712.

Engel, C.G., and Fisher, R.L., 1975. Granitic to ultramafic rock complexes of the Indian Ocean Ridge system, western Indian Ocean. *Geol. Soc. Am. Bull.,* 86:1553-1578.

Gerlach, D.C., Avé Lallemant, H.G., and Leeman, W.P., 1981. An island arc origin for the Canyon Mountain ophiolite complex, eastern Oregon, U.S.A. *Earth Planet. Sci. Lett.,* 53:255-265.

Gerlach, D.C., Stormer, J.C., and Mueller, P.A., 1987. Isotopic geochemistry of Fernando de Noronha. *Earth Planet. Sci. Lett.,* 85:129-144.

Gunn, B.M., and Roobol, M.J., 1977. Geochemistry of the igneous rocks. *In* Aumento, F., Melson, W.G., et al., *Init. Repts. DSDP,* 37: Washington (U.S. Govt. Printing Office), 735-755.

Hajash, A., 1975. Hydrothermal processes along Mid-Ocean Ridges: an experimental investigation. *Contrib. Mineral. Petrol.,* 53:205-226.

Hajash, A., and Archer, P., 1980. Experimental seawater/basalt interactions: effects of cooling. *Contrib. Mineral. Petrol.,* 75:1-13.

Hamelin, B., Dupre, B., and Allegre, C.J., 1984. Lead-strontium isotopic variations along the East Pacific Rise and the Mid-Atlantic Ridge: a comparative study. *Earth Planet. Sci. Lett.,* 67:340-350.

Hekinian, R., Bideau, D., Francheteau, J., Cheminée, J.L., Armijo, R., Lonsdale, P., and Blum, N., 1993. Petrology of the East Pacific Rise crust and upper mantle exposed in the Hess Deep (eastern equatorial Pacific). *J. Geophys. Res.,* 98:8069-8094.

Henderson, P., 1982. *Inorganic Geochemistry:* Oxford (Pergamon Press).

Humphris, S.E., and Thompson, G., 1978. Hydrothermal alteration of oceanic basalts by seawater. *Geochim. Cosmochim. Acta,* 42:107-125.

Humphris, S.E., Thompson, G., Schilling, J.G., and Kingsley, R.H., 1985. Petrological and geochemical variations along the Mid-Atlantic Ridge between 46°S and 32°S: influence of the Tristan da Cunha mantle plume. *Geochim. Cosmochim. Acta,* 49:1445-1464.

Jaques, A.L., and Chappell, B.W., 1980. Petrology and trace element geochemistry of the Papuan ultramafic belt. *Contrib. Mineral. Petrol.,* 75:55-70.

Leterrier, J., 1985. Mineralogical, geochemical and isotopic evolution of two Miocene mafic intrusions from the Zagros (Iran). *Lithos,* 18:311-329.

McCulloch, M.T., Gregory, R.T., Wasserburg, G.J., and Taylor, H.P., Jr., 1980. A neodynium, strontium, and oxygen isotopic study of the Cretaceous Samail ophiolite and implications for the petrogenesis and seawater-hydrothermal alteration of oceanic crust. *Earth Planet. Sci. Lett.,* 46:201-211.

Mével, C, and Cannat, M., 1991. Lithospheric stretching and hydrothermal processes in oceanic gabbros from slow-spreading ridges. *In* Peters, T., Nicolas, A., and Coleman, RJ. (Eds.), *Ophiolite Genesis and Evolution of the Oceanic Lithosphere.* Petrol. Struct. Geol., 5:293-312.

Meyer, P.S., Dick, H.J.B., and Thompson, G., 1989. Cumulate gabbros from the Southwest Indian Ridge, 54°S-7°16'E: implications for magmatic processes at a slow spreading ridge. *Contrib. Mineral. Petrol.,* 103:44-63.

Michard, A., and Albarede, F., 1985. Hydrothermal uranium uptake at ridge crests. *Nature,* 317:244-245.

Miyashiro, A., and Shido, F., 1980. Differentiation of gabbros in the mid-Atlantic ridge near 24°N. *Geochem. J.,* 14:145-154.

Mottl, M.J., and Holland, H.D., 1978. Chemical exchange during hydrothermal alteration of basalt by seawater, I. Experimental results for major and minor components of seawater. *Geochim. Cosmochim. Acta,* 42:1103-1115.

Murillas, J., Mougenot, D., Boillot, G., Comas, M.C., Banda, E., and Mauffret, A., 1990. Structure and evolution of the Galicia Interior basin (Atlantic western Iberian continental margin). *Tectonophysics,* 184:297-319.

O'Nions, R.K., Hamilton, P.J., and Evensen, N.M., 1977. Variations in $^{143}Nd/^{144}Nd$ and $^{87}Sr/^{86}Sr$ in oceanic basalts. *Earth Planet. Sci. Lett.,* 34:13-22.

Phelps, D., and Avé Lallemant, H.G., 1980. The Sparta ophiolite complex. northeast Oregon: a plutonic equivalent to low K_2O island-arc volcanism. *Am. J. Sci.,* 280A:345-358.

Pinheiro, L.M., Whitmarsh, R.B., and Miles, P.R., 1992. The ocean-continent boundary off the western continental margin of Iberia, II. Crustal structure in the Tagus Abyssal Plain. *Geophys. J.,* 109:106-124.

Richardson, S.H., Erlank, A.J., Duncan, A.R., and Reid, D.L., 1982. Correlated Nd, Sr and Pb isotope variation in Walvis Ridge basalts and implications for the evolution of their mantle source. *Earth Planet. Sci. Lett.,* 59:327-342.

Robinson, P.T., Dick, H.J.B., and Von Herzen, R.P., 1991. Metamorphism and alteration in oceanic layer 3: Hole 735B. *In* Von Herzen, R.P., Robinson, P.T., et al., *Proc. ODP, Sci. Results,* 118: College Station, TX (Ocean Drilling Program), 541-552.

Rollinson, H.R., 1993. *Using Geochemical Data: Evaluation, Presentation, Interpretation:* London (Longman).
Sawyer, D.S., Whitmarsh, R.B., Klaus, A., et al., 1994. *Proc. ODP, Init. Repts.,* 149: College Station, TX (Ocean Drilling Program).
Schilling, J.-G., Zajac, M, Evans, R., Johnston, T., White, W., Devine, J.D., and Kingsley, R., 1983. Petrologic and geochemical variations along the Mid-Atlantic ridge from 29°N to 73°N. *Am. J. Sci.,* 283:510-586.
Serri, G., 1981. The petrochemistry of ophiolite gabbroic complexes: a key for the classification of ophiolites into low-Ti and high-Ti types. *Earth Planet. Sci. Lett.,* 52:203-212.
Seyfried, W.E., and Bischoff, J.L., 1979. Low temperature basalt alteration by seawater: an experimental study at 70°C and 150°C. *Geochim. Cosmochim. Acta,* 43:1937-1947.
Srivastava, S.P., Schouten, H., Roest, W.R., Klitgord, K.D., Kovacs, L.C., Verhoef, J., and Macnab, R., 1990. Iberian plate kinematics: a jumping plate boundary between Eurasia and Africa. *Nature,* 344:756-759.
Stacey, J.S., and Kramers, J.D., 1975. Approximation of terrestrial lead isotope evolution by a two-stage model. *Earth Planet. Sci. Lett.,* 26:207-221.
Sun, S.-S., 1980. Lead isotopic study of young volcanic rocks from mid-ocean ridges, ocean islands and island arcs. *Philos. Trans. R. Soc. London A,* 297:409-445.
Sun, S.-S., and McDonough, W.F., 1989. Chemical and isotopic systematics of oceanic basalts: implications for mantle composition and processes. *In* Saunders, A.D., and Norry, M.J. (Eds.), *Magmatism in the Ocean Basins.* Geol. Soc. Spec. Publ. London, 42:313-345.
Tatsumoto, M., 1978. Isotopic composition of lead in oceanic basalt and its implication to mantle evolution. *Earth. Planet. Sci. Lett.,* 38:63-87.
Thompson, G., 1973. Trace element distributions in fractionated oceanic rocks, 2. Gabbros and related rocks. *Chem. Geol.,* 12:99-111.
Tiezzi, L.J., and Scott, R.B., 1980. Crystal fractionation in a cumulate gabbro, Mid-Atlantic Ridge, 26°N. *J. Geophys. Res.,* 85:5438-5454.
Vogt, P.R., and Perry, R.K., 1981. North Atlantic Ocean: bathymetry and plate tectonic evolution. *Geol. Soc. Am., Map and Chart Ser.,* MC-35.
Weis, D., 1983. Pb isotopes in Ascension Island rocks: oceanic origin for the gabbroic to granitic plutonic xenoliths. *Earth Planet. Sci. Lett.,* 62:273-282.
Weis, D., Demaiffe, D., Cauët, S., and Javoy, M., 1987. Sr, Nd, O and H isotopic ratios in Ascension Island lavas and plutonic inclusions: cogenetic origin. *Earth Planet. Sci. Lett.,* 82:255-268.
Weis, D., and Frey, F.A., 1991. Isotope geochemistry of Ninetyeast Ridge basement basalts: Sr, Nd, and Pb evidence for involvement of the Kerguelen hot spot. *In* Weissel, J., Peirce, J., Taylor, E., Alt, J., et al., *Proc. ODP, Sci. Results,* 121: College Station, TX (Ocean Drilling Program), 591-610.
White, W.M., and Hofmann, A.W., 1982. Sr and Nd isotope geochemistry of oceanic basalts and mantle evolution. *Nature,* 296:821-825.
Whitmarsh, R.B., Miles, P.R., and Mauffret, A., 1990. The ocean-continent boundary off the western continental margin of Iberia, I. Crustal structure at 40°30'N. *Geophys. J. Int.,* 103:509-531.
Whitmarsh, R.B., Pinheiro, L.M., Miles, P.R., Recq, M., and Sibuet, J.C., 1993. Thin crust at the western Iberia ocean-continent transition and ophiolites. *Tectonics,* 12:1230-1239.
Wilson, R.C.L., Hiscott, R.N., Willis, M.G., and Gradstein, P.M., 1989. The Lusitanian Basin of west-central Portugal: Mesozoic and Tertiary tectonic, stratigraphic and subsidence history. *In* Tankard, A.J., and Balkwill, H.R. (Eds.), *Extensional Tectonics and Stratigraphy of the North Atlantic Margins.* AAPG Mem., 46:341-361.
Yardley, B.W., 1989. *An Introduction to Metamorphic Petrology:* Essex, England (Longman Earth Sci. Ser.).
Zindler, A., Jagoutz, E., and Goldstein, S., 1982. Nd, Sr and Pb isotopic systematics in a three-component mantle: a new perspective. *Nature,* 298:519-523.

Date of initial receipt: 1 December 1994
Date of acceptance: 14 June 1995
Ms 149SR-221

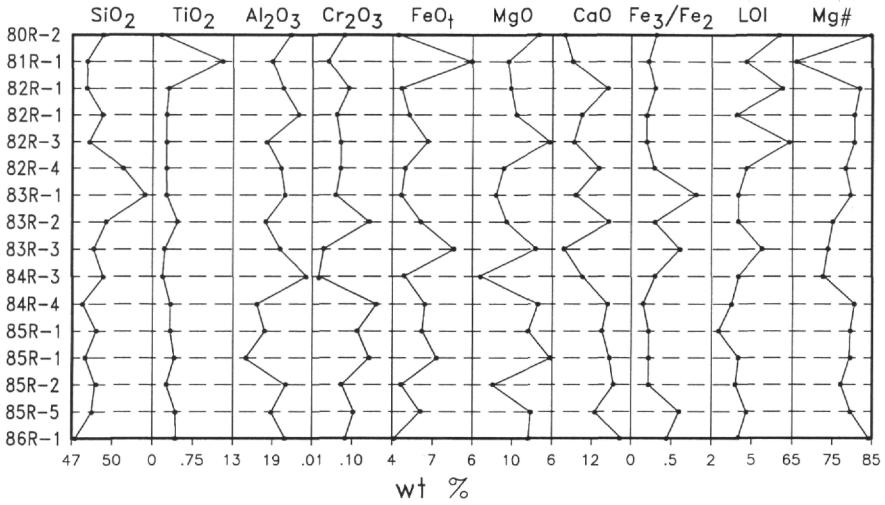

Figure 8. Variation with depth of major element composition (calculated dry) in the metamorphosed mafic rocks in Hole 900A. Fe_3/Fe_2 is the oxidation ratio and shorthand for Fe_2O_3/FeO. The Mg# is based on FeO = .85 FeO_t. The abbreviated core numbers correspond to the samples listed in Table 3 and are in order of depth, although spacing between samples is not uniform. The compositional data for this figure have been recalculated from Table 3.

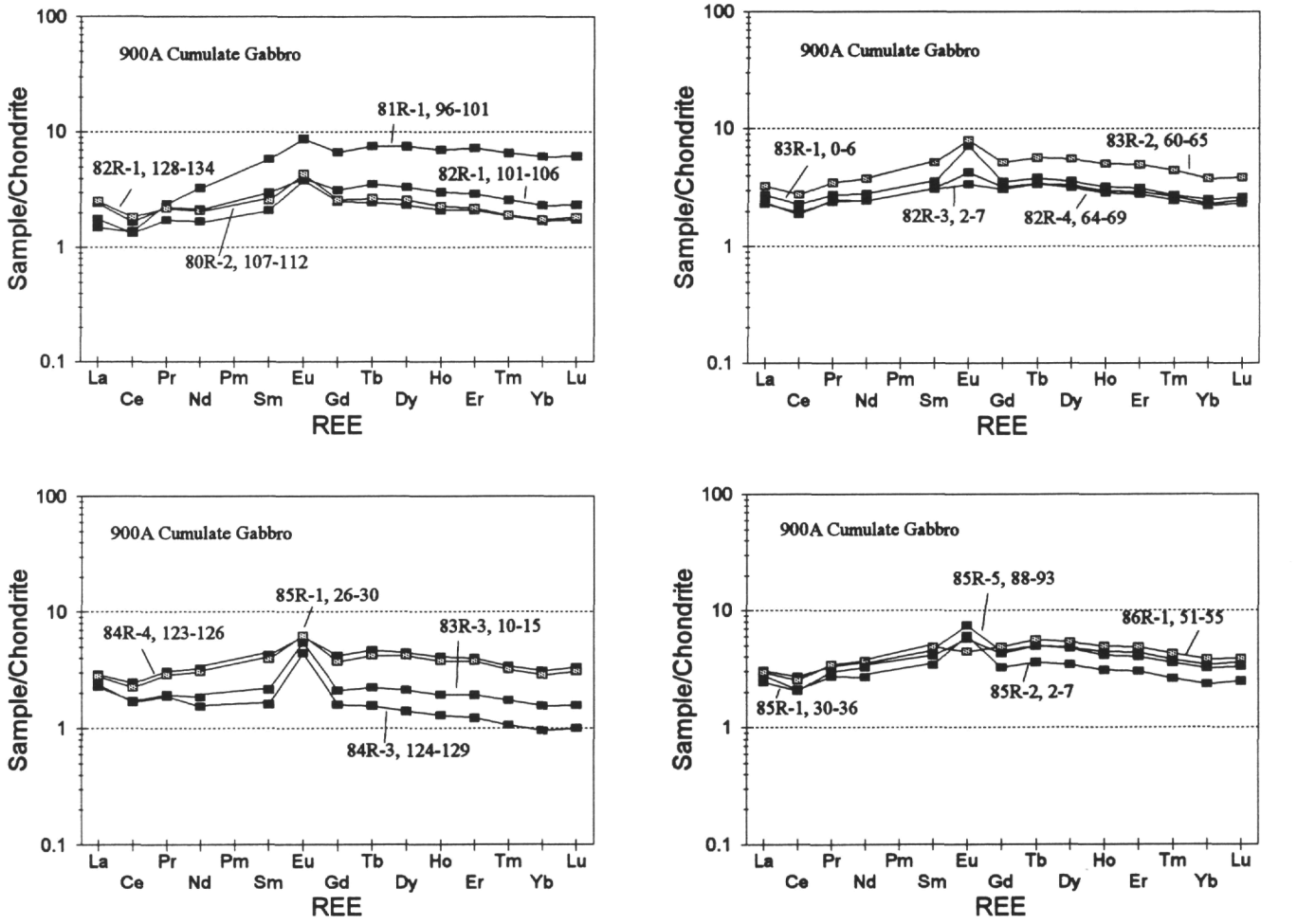

Figure 9. Chondrite normalized REE patterns for the metamorphosed mafic rocks showing typical flat patterns near 2X-4X chondrite and small positive Eu anomalies. A distinctly different N-MORB-type pattern is shown by Sample 900A-81R-01, 96-101 cm. The REEs are listed in order of increasing atomic number. Chondrite values used for normalization are taken from Anders and Grevesse (1989) and multiplied by 1.36 to maintain consistency with older chondrite normalization values.

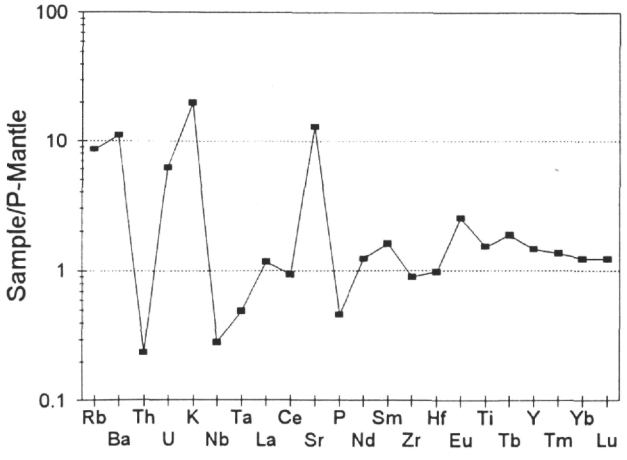

Figure 10. A spider diagram with a spidergram pattern for the typical Hole 900A cumulate gabbro using a modified elemental sequence and normalizing values from Sun and McDonough (1989). The immobile REEs and HFSEs have low concentrations similar to primitive mantle, indicating very little magma retention, but strong enrichment in the LILE (Rb, Ba, K, and Sr).

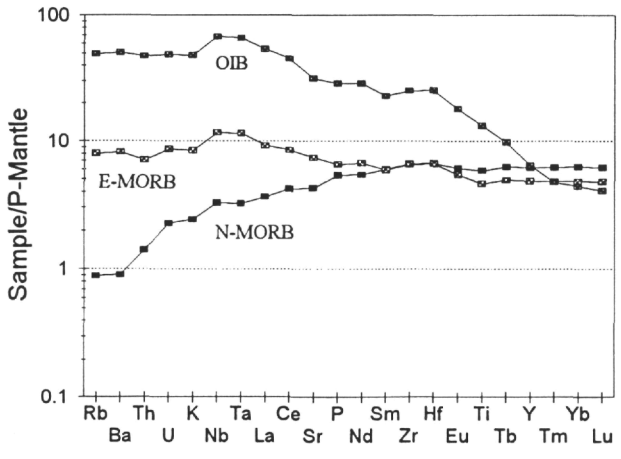

Figure 11. A spider diagram with spidergram patterns for typical N-MORB, E-MORB, and OIB using a modified elemental sequence and normalizing values for P-Mantle (primitive mantle) from Sun and McDonough (1989).

Table 4. Isotopic data for Hole 900A cumulate gabbros.

	Core 81R	Core 82R	Core 85R
Rb	4.64	4.79	1.25
Sr	209	297	191
$^{87}Rb/^{86}Sr$ (0)	0.0642465	0.0466718	0.0189378
$^{87}Sr/^{86}Sr$ (0)	0.705079	0.705028	0.704505
$^{87}Sr/^{86}Sr$ (136.4)	0.70495	0.70494	0.70447
Pb	0.69	0.34	0.30
U	0.75	0.16	0.17
$^{206}Pb/^{204}Pb$ (0)	19.138	18.598	18.740
$^{206}Pb/^{204}Pb$ (136.4)	17.653	17.962	17.971
$^{207}Pb/^{204}Pb$ (0)	15.690	15.645	15.617
$^{207}Pb/^{204}Pb$ (136.4)	15.618	15.614	15.580
$^{208}Pb/^{204}Pb$ (0)	38.09	37.89	38.06
Sm	1.16	0.51	0.81
Nd	2.01	1.27	1.96
$^{147}Sm/^{144}Nd$ (0)	0.3490	0.2428	0.2499
$^{143}Nd/^{144}Nd$ (0)	0.513303	0.513047	0.513008
ε Nd (0)	12.9	7.98	7.22
$^{143}Nd/^{144}Nd$ (136.4)	0.51299	0.51283	0.51279
ε Nd (136.4)	10.32	7.18	6.29
$\delta^{18}O$	4.01	4.22	3.48

Note: elements Rb, Sr, Pb, U, Sm, and Nd are expressed in ppm.

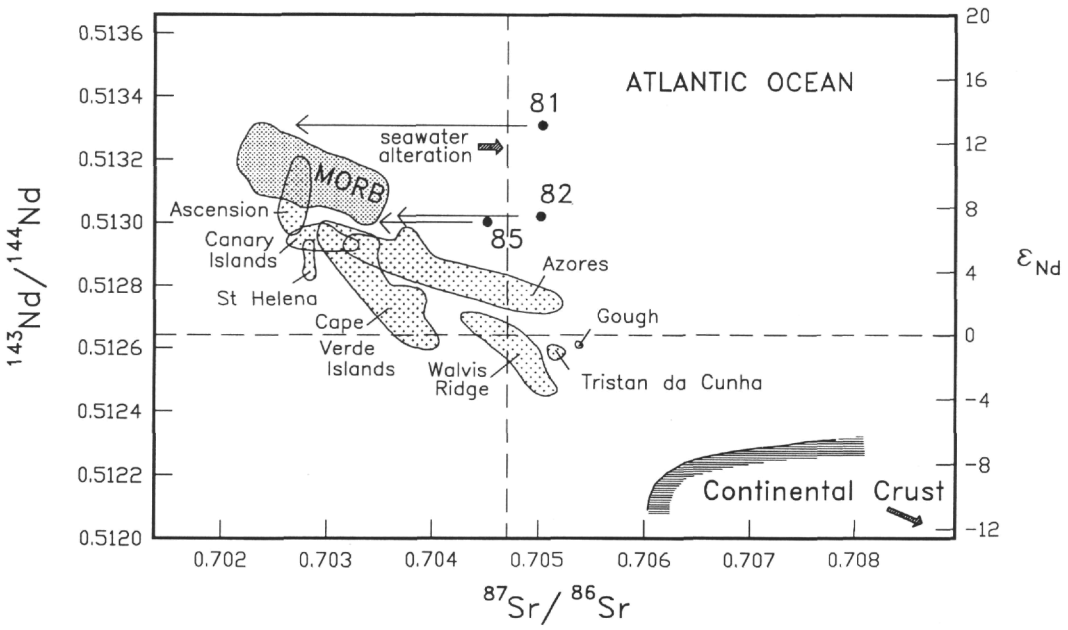

Figure 12. The measured Nd-Sr isotope systematics for samples from Cores 149-900A-81R, 900A-82R, and 900A-85R plotted relative to MORB and OIB from the Atlantic Ocean. Isotopic data for Iceland and Fernando de Noronha were not plotted because of significant data overlap with other islands already plotted on the Nd-Sr diagram. The high $^{143}Nd/^{144}Nd$ ratios of the three Hole 900A samples indicate MORB affinities. Seawater alteration has increased the $^{87}Sr/^{86}Sr$ ratios in the direction indicated by the arrow. Isotopic data for Atlantic Ocean MORB and OIB were obtained from Cohen and O'Nions, 1982; Dosso et al., 1993; Davies et al., 1989; O'Nions et al., 1977; Richardson et al., 1982; Weis et al., 1987; White and Hofmann, 1982; and Zindler et al., 1982.

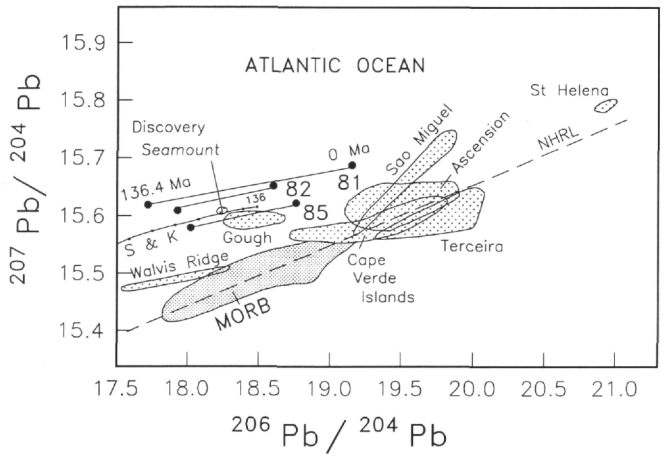

Figure 13. A $^{207}Pb/^{204}Pb$ vs. $^{206}Pb/^{204}Pb$ isotope diagram showing the relationship of the three Hole 900A samples relative to MORB and OIB from the Atlantic Ocean. Although the relatively high $^{207}Pb/^{204}Pb$ values of the Hole 900A samples might appear to allow an OIB origin, the very high ϵ_{Nd} (Fig. 12) undoubtedly point to a depleted mantle source. In addition, we have plotted both the measured Pb values and the age-corrected in situ decay values. The correction is unusually large because of the enrichment in U from seawater alteration. The real corrected values at 136.4 Ma for the Hole 900A rocks are most probably in between the measured and age-corrected values here plotted. The high $^{207}Pb/^{204}Pb$ values relative to recent Atlantic MORB probably reflect seawater alteration also. Correction for 136.4 Ma MORB would result in only a very small displacement toward the lower left corner. The two-stage lead isotope curve of Stacey and Kramers (1975) is shown by the line labeled S & K and marked with dots 100 Ma apart; except for the farthest-right dot, which represents 136 Ma. The dot immediately to its left is at 200 Ma. The far-left dot on the S & K curve is at 700 Ma. This curve represents the average evolution curve for continental crust. The Hole 900A rocks, at 136.4 Ma, are distinctly less radioactive than corresponding continental crust of that age, which confirms the oceanic origin of these rocks. Isotopic data for Atlantic Ocean MORB and OIB were obtained from Cohen and O'Nions, 1982; Gerlach et al., 1987; Hamelin et al., 1984; Richardson et al., 1982; Sun, 1980; Weis, 1983; and Zindler et al., 1982.

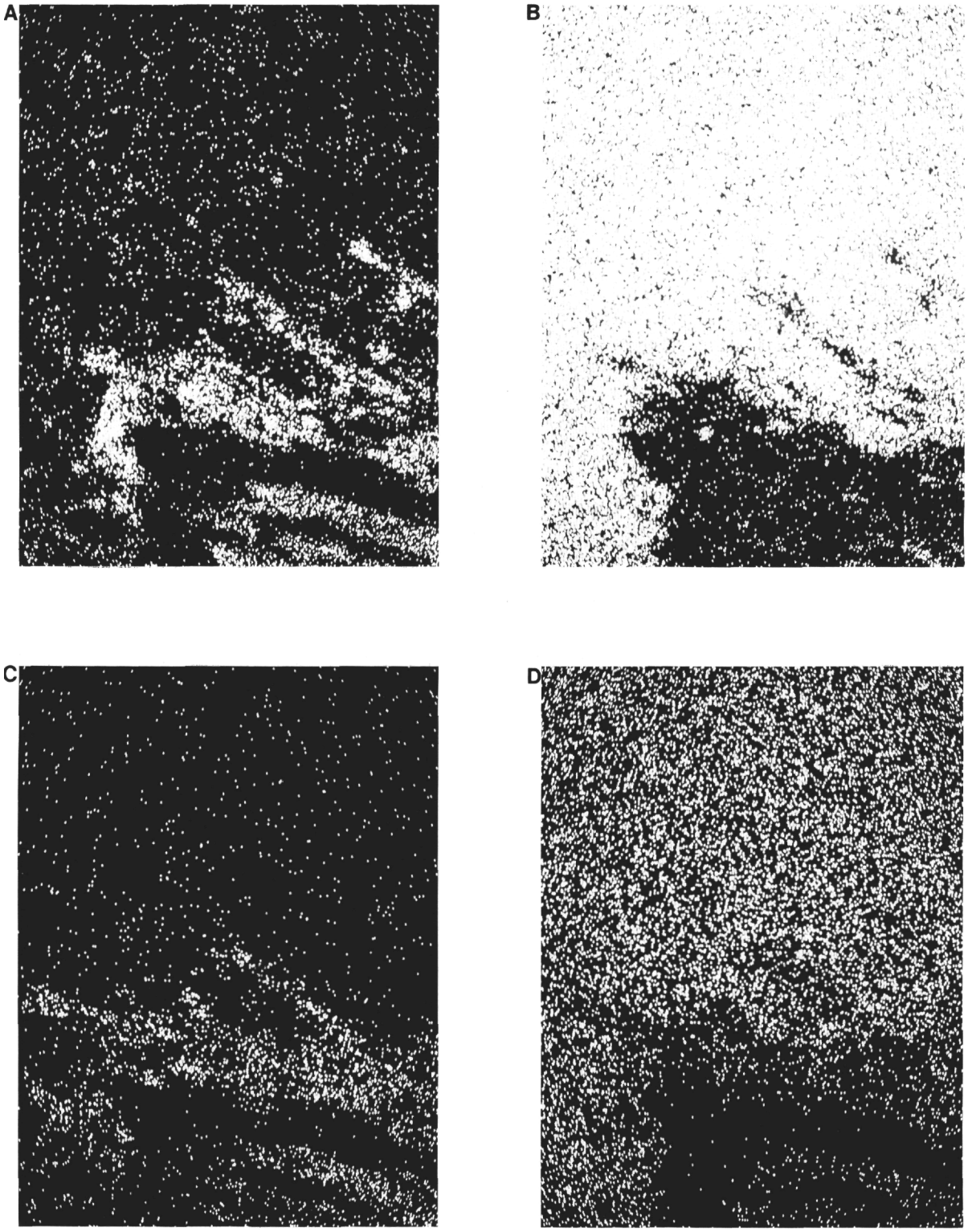

Figure 14. Microprobe elemental maps of a brown fibrous alteration patch within a plagioclase porphyroclast in Sample 149-900A-83R-2, 60–65 cm. The photos have a long dimension of roughly 160 µm and increasing brightness marks increasing concentrations. **A.** The K concentrations occur in patches with irregular to fibrous shapes associated with a nonpleochroic fibrous amphibole. **B.** The concentration of Ca marks the unaltered surrounding porphyroclast. **C.** The Mg and Fe concentrations roughly coincide with the K concentration in the brown-stained alteration patch, except for one of the K-rich alteration fibers near the center of the photograph. **D.** The Al concentration coincides with Ca concentration in the unaltered surrounding plagioclase porphyroclast.

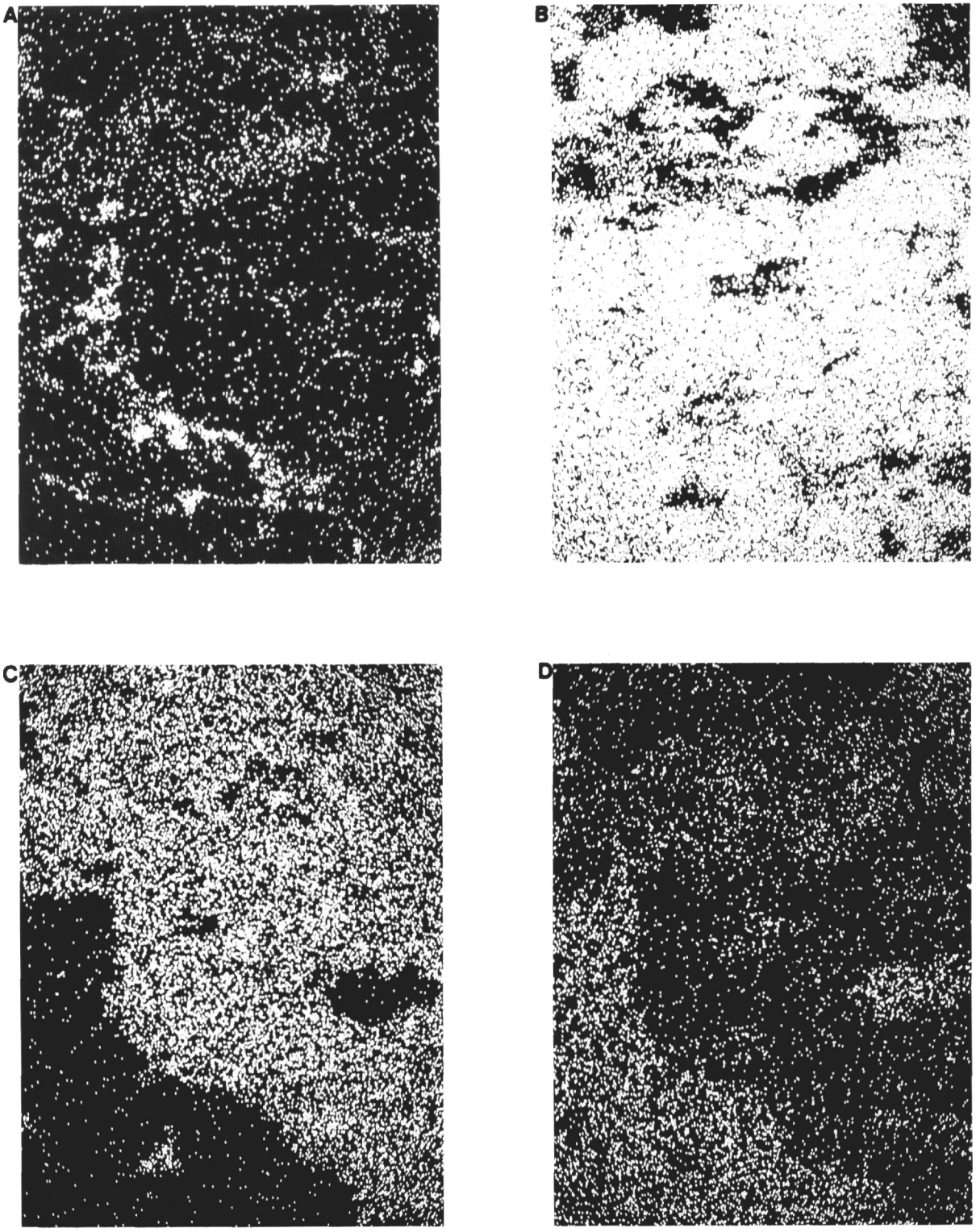

Figure 15. Microprobe elemental maps of a patchy grain boundary alteration band between recrystallized plagioclase and clinopyroxene in Sample 149-900A-83R-2, 60-65 cm. The photos have a long dimension of roughly 160 µm and increasing brightness marks increasing concentrations. **A.** The K concentration is patchy and does not correlate well with the concentration of any other analyzed element. **B.** The Ca concentration is high in both plagioclase and clinopyroxene and slightly lower in the irregular K-rich region. **C.** The Mg concentration, and a similar Fe concentration, marks the position of a clinopyroxene crystal. **D.** The Al concentration marks the position of a plagioclase crystal.

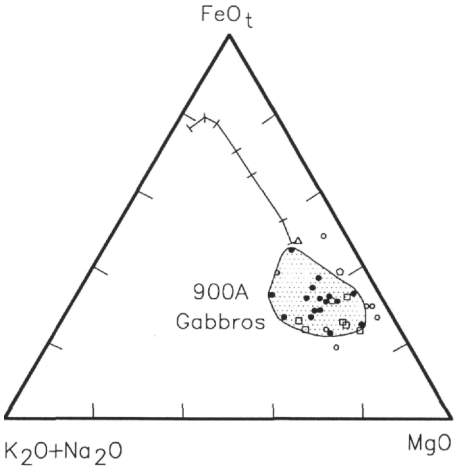

Figure 16. When the metamorphosed mafic rocks (solid circles) are plotted on an AFM diagram, they fall below the M (MgO) end of the Skaergaard trend (crossed line) in a region characterized by cumulate gabbros. Cumulate gabbros from a variety of tectonic provinces are plotted for comparison: open circles = cumulate gabbros from ophiolites (Beccaluva et al., 1977; Phelps and Avé Lallemant, 1980; and Jaques and Chappell, 1980); squares = cumulate gabbros from the Southwest Indian Ridge (Meyer et al., 1989); pentagon = cumulate gabbro from the Mid-Atlantic Ridge (Tiezzi and Scott, 1980); triangle = N-MORB (Humphris et al., 1985). The Hole 900A sample, which plots separately at the top of the field near N-MORB, is Sample 149-900A-81R-1, 96-101 cm; it contains opaque minerals and higher concentrations of incompatible elements.

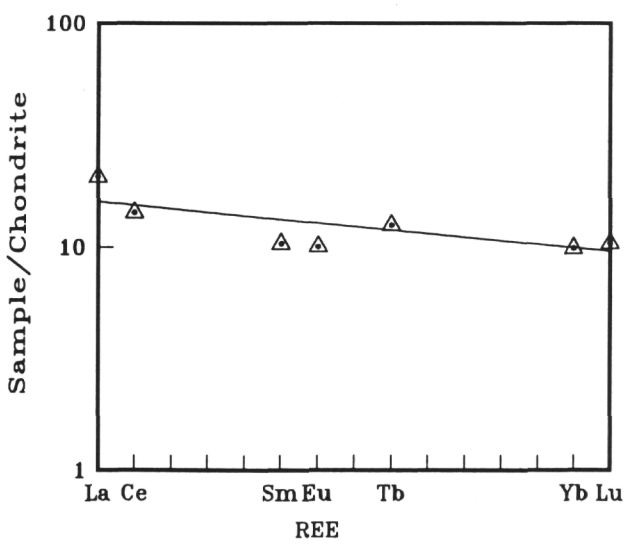

Figure 17. The estimated REE pattern for the typical Hole 900A parental magma resembles a transitional MORB REE pattern. The chondrite values used for normalization are taken from Anders and Grevesse (1989) and multiplied by 1.36 to maintain consistency between newer carbonaceous chondrite normalization values and older chondrite normalization values.